agronomy

MDPI

Article

Subsurface Drip Irrigation with Emitters Placed at Suitable Depth Can Mitigate N_2O Emissions and Enhance Chinese Cabbage Yield under Greenhouse Cultivation

Amar Ali Adam Hamad [1], Qi Wei [1,*], Lijun Wan [2], Junzeng Xu [1,3], Yousef Alhaj Hamoud [1], Yawei Li [1] and Hiba Shaghaleh [4]

[1] College of Agricultural Science and Engineering, Hohai University, Nanjing 210098, China; d2018008@hhu.edu.cn (A.A.A.H.); xjz481@hhu.edu.cn (J.X.); yousef-hamoud11@hhu.edu.cn (Y.A.H.); yaweizx@hhu.edu.cn (Y.L.)
[2] Planning and Planning Department, Yixing Water Resources Bureau, Wuxi 214200, China; zipper5@163.com
[3] State Key Laboratory of Hydrology-Water Resources and Hydraulic Engineering, Hohai University, Nanjing 210098, China
[4] College of Chemical Engineering, Nanjing Forestry University, Nanjing 210037, China; hiba-shaghaleh@njfu.edu.cn
* Correspondence: weiqi8855116@163.com; Tel.: +86-258-378-6016

Abstract: Agricultural practices, such as applying excessive water and nitrogen fertilizer to increase the crop yield, can be a significant source of greenhouse gas emissions (GHGs). Therefore, techniques and proper management are needed to mitigate these emissions without yield reduction. The experiment used three subsurface drip irrigation (SDI) depths with emitters buried at 0.05, 0.10, and 0.15 m below the soil surface, along with two nitrogen fertilizer (Urea, N > 46.2%) application levels of 300 kg N ha^{-1} (N_{300}) and 240 kg N ha^{-1} (N_{240}) to investigate the effect of vertical and horizontal water and fertilizer distribution on N_2O emissions under different SDI techniques in greenhouse conditions. The results indicated that soil N_2O emissions from SDI_{10} and SDI_{15} decreased by 7.06% and 10.69%, respectively, compared to SDI_5. N_2O, WFPS, NH_4^+-N, and NO_3^--N were significantly reduced with the increased radial distance from the emitter. N_2O was positively correlated to WFPS and NH_4^+-N while negatively correlated to NO_3^--N. The NH_4^+-N and NO_3^--N concentrations decreased with depth and increased with fertilization events. Furthermore, N_2O, WFPS, NH_4^+-N, and NO_3^--N were increased under N_{300} compared to N_{240} ($p > 0.05$). The findings demonstrated that the Chinese cabbage yield was significantly enhanced under SDI_{15} compared to SDI_5 and SDI_{10}. Furthermore, N_{300} can increase the cabbage yield more than N_{240} among all treatments.

Keywords: N_2O emissions; water distribution; ammonium nitrogen; nitrate nitrogen; subsurface drip irrigation (SDI)

check for updates

Citation: Hamad, A.A.A.; Wei, Q.; Wan, L.; Xu, J.; Hamoud, Y.A.; Li, Y.; Shaghaleh, H. Subsurface Drip Irrigation with Emitters Placed at Suitable Depth Can Mitigate N_2O Emissions and Enhance Chinese Cabbage Yield under Greenhouse Cultivation. *Agronomy* **2022**, *12*, 745. https://doi.org/10.3390/agronomy12030745

Received: 12 February 2022
Accepted: 17 March 2022
Published: 20 March 2022

1. Introduction

One of the three major greenhouse gases (GHGs), nitrous oxide (N_2O), has a global warming potential 265 times that of an equivalent amount of carbon dioxide (CO_2) over 100 years [1]. Agricultural practices such as water and nitrogen (N) management can contribute to GHGs emissions [2]. Agricultural soils are the most significant sources of N_2O, contributing about 60–80% of the total global anthropogenic N_2O emitted into the atmosphere [3,4]. The microbiological processes of nitrification produce N_2O under aerobic conditions and denitrification under anaerobic conditions, which are controlled by several factors, including soil moisture (θ), soil temperature, agricultural activities, and the availability of C, O_2, and mineral N [5]. Therefore, proper water and fertilizer management measures are important to reduce soil N_2O emissions. Research on this topic will provide essential guidance on how we can slow down the global greenhouse effect.

(θ) is one of the most critical factors affecting N_2O emissions since the level and distribution of water in the soil can provide suitable or unsuitable conditions for microorganisms, thereby affecting the activity of soil microorganisms and the discharge of N_2O [6,7]. Therefore, managing θ is the most important key to mitigating N_2O emissions from agricultural soil. Several studies have investigated the effects of θ on N_2O emissions in a greenhouse environment. For example, Ye et al. [8] demonstrated that θ was the main factor affecting soil N_2O emissions. Edwards et al. [9] stated that lesser N_2O emissions occurred under SDI and DI.

Growers in China are still using high nutrient and water inputs to obtain a higher yield [10,11]. Excessive irrigation watering and N fertilizer application have caused several environmental problems, including GHGs emissions. In contrast, low mineral nutrition affects overall plant growth [12]. SDI is a more effective water management method than other irrigation methods. It has numerous benefits, including water savings, easy fertigation, less surface runoff, and deep percolation [13]. Many studies have demonstrated that different irrigation methods have different effects on θ distribution, and thus, N_2O emissions. For example, Sanchez-Martin et al. [14] found that N_2O emissions were influenced by the irrigation system and the mineral fertilizer applied. Peaks in N_2O are generally driven by fertilizer application or irrigation. In a pair of studies, SDI markedly reduced N_2O emissions compared with DI [9,15]. Reducing surface soil wetting through SDI reduces N_2O emissions [16,17]. To the best of our knowledge, barely any previous studies have investigated the dynamics of soil water and N and their effects on N_2O emissions under different depths of SDI, or investigated the influence of the horizontal water and nutrient distribution on N_2O emissions. Thus, we hypothesized that SDI with emitters placed at a suitable depth could mitigate N_2O emissions and enhance crop yield. The objectives were: to study the differences in soil moisture, nitrogen, and N_2O emissions under different depths of SDI irrigation; to reveal the response of soil N_2O emissions to water and nitrogen dynamics; to explore the appropriate buried depth of SDI that provides high-efficiency N_2O reduction while maintaining a high crop yield.

2. Materials and Methods

2.1. Descriptions of Study Area

Greenhouse production of Chinese cabbage [*Brassica rapa* subsp. *pekinensis* (Lour.) Hanelt] under natural light conditions was carried out at the Water-Saving Park of Hohai University, Nanjing, Jiangsu province, China (31°95′ N, 118°83′ E; elevation 15 m AMSL). The climate of the study area is characterized as humid and is under the influence of the East Asian Monsoon. The mean temperature in the greenhouse was 21.0 °C, and the mean relative humidity was 58% during the experimental period. The experimental plots were manually prepared with conventional tillage to a depth of 0.30 m. The soil of the experimental field was clay loam. The soil's chemical and physical properties were described in our previous work [18].

2.2. Experimental Design

The experiment set up two factors: three SDI emitter depths of 0.05, 0.10, and 0.15 m (SDI_5, SDI_{10}, and SDI_{15}), factorially combined with two levels of nitrogen fertilizer as urea (300 kg N ha^{-1} and 240 kg N ha^{-1}). The former N fertilization rate was locally recommended for Chinese cabbage production. We created a completely randomized block design with six treatments, named $SDI_5 + N_{300}$, $SDI_5 + N_{240}$, $SDI_{10} + N_{300}$, $SDI_{10} + N_{240}$, $SDI_{15} + N_{300}$, and $SDI_{15} + N_{240}$. Detailed information on the experimental layout is shown in Figure 1, with the experimental layout of the subsurface drip irrigation system given as the whole treatment layout (Figure 1a), plot layout (Figure 1b), and horizontal distances from the dripper point (Figure 1c). Before the start of the experiment, we inserted waterproof material with a thickness of 8 mm and height of 0.50 m on the ridge of two adjacent plots to reduce the water and N transport between the two adjacent plots as much as possible and improve the accuracy and reliability of the research results. Each treatment was replicated three times, resulting in 18 plots. Six lateral pipelines with a lateral spacing of 0.20 m were arranged on each plot, and three plants were arranged on each pipeline spaced 0.40 m apart (Figure 1b). Our purpose was to ensure that sufficient soil and gas samples with similar characteristics could be collected at different crop growth stages. The soil was thoroughly mixed to raise the beds manually. Every two adjacent plots were separated by a ridge 0.25 m thick. All plots received the same amount of water during the growing season: 0.15 m^3 per plot (892.8 m^3 ha^{-1}) with a flow rate of 3 L h^{-1}. The treatments were irrigated three times over the entire growing period, at 20-day intervals. Irrigation water was delivered to the plots via a gravity drip system. At the upper end of each plot, a tank to store irrigation water (0.05 m^3) was installed at the height of 2 m. Nitrogen fertilizer was mixed with irrigation water in the water tank, with each treatment having a separate drip line.

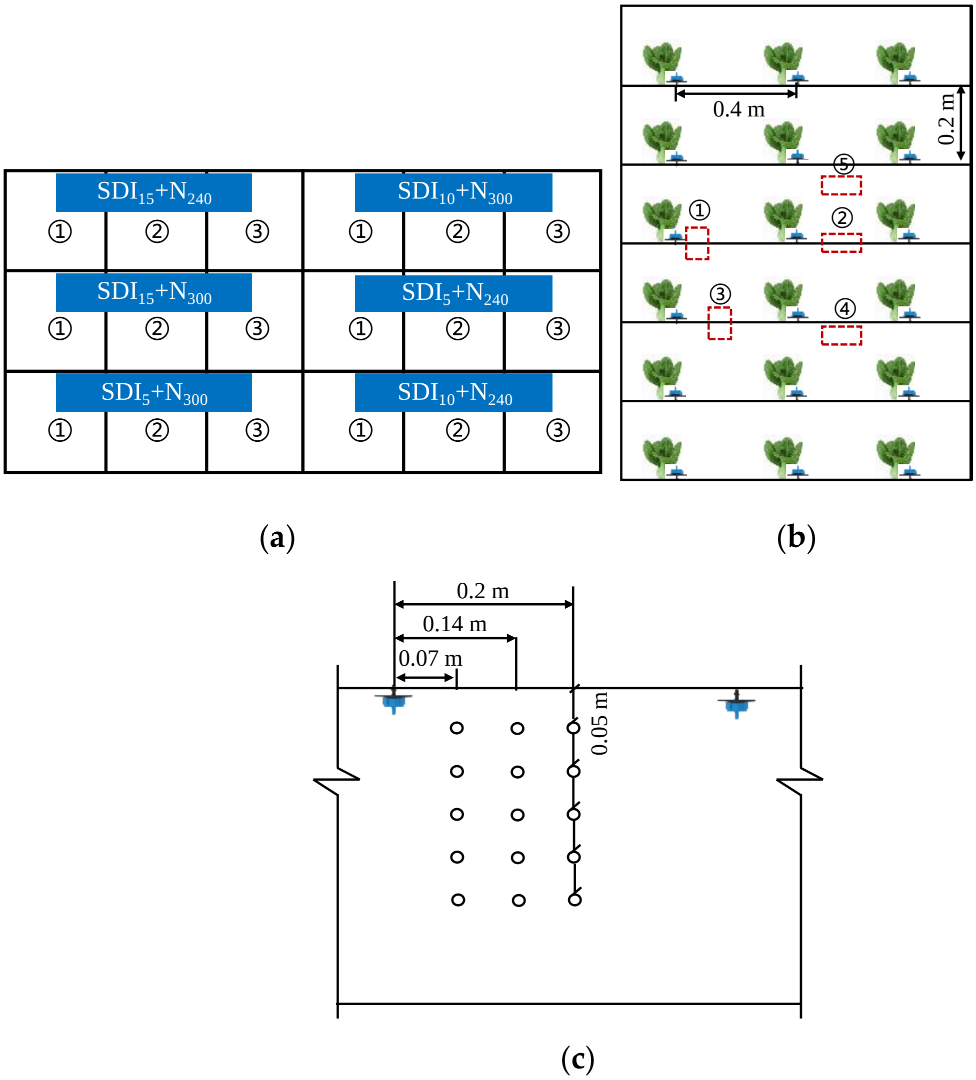

Figure 1. Experimental layout of subsurface drip irrigation system. Treatment layout (**a**), plot layout (**b**), and horizontal distances from the dripper point (**c**).

2.3. Measurement of θ, $NH_4{}^+$-N, and $NO_3{}^-$-N

In each treatment plot, 5–10 g soil samples were collected using a 0.05-m diameter hand auger from varying depths (0.05, 0.10, 0.15, 0.20, and 0.25 m) and at three horizontal distances from the emitter (0.07, 0.14, and 0.20 m). The samples were immediately taken to the laboratory to determine θ by the traditional drying method (105 °C, 8 h). The water-filled pore space (WFPS) was then determined by dividing the volume of gravimetric water by the soil's total porosity (ϕ), itself determined by calculating soil's bulk density by the following relationship:

$$\text{Soil porosity} = 1 - \frac{\text{BD}}{\text{PD}} \quad (1)$$

where BD and PD are the bulk density and particle density, respectively. The particle density was estimated to be 2.65 g cm^{-3} [19]. A further 10 g of soil was extracted with 1 M KCl solution (50 mL), shaken at 300 rpm for 1 h, and filtered through filter paper (Whatman no. 42). Using a colorimetric method [2], the soil ammonium (NH_4^+-N) nitrate (NO_3^--N) content in the filtrate was measured.

2.4. Gas Sampling and Analyses

Before the experiment, five rectangular stainless-steel chamber bases were mounted in each plot at a depth of approximately 0.05 m and at different horizontal distances from the emitters. The bases served to mitigate lateral gas diffusion during gas sampling and remained open throughout the crop growing period except during gas sampling (Figure 1b). During the growing season, the bases of the chambers were left to prevent soil disruption. The 0.20 × 0.10 × 0.20 m (length × width × height) chambers were made of polyvinyl chloride and fitted with thermometers (Figure 2). The chambers were closed by placing them into rings made of stainless steel, which were sunk into the soil. The chambers were coated by wrapping them in a layer of heat insulation material to reduce the influence of heat transfer induced by ambient temperature. Furthermore, to minimize potential soil temperature, soil moisture, and micro-climate modification of the sampling area, the static chambers were removed from the bases immediately after gas sampling. Gas samples were obtained using 10-mL syringes linked to the chambers by a pipe and valve system. Three gas samples were collected from each chamber at 10-min intervals between 10:00 and 10:30 a.m. Every 10 min, the air temperatures inside the chambers were recorded using thermometers. A gas chromatograph (Agilent 7890A, Santa Clara, CA, USA) was used to analyze the N_2O concentrations using an electron capture detector (ECD).

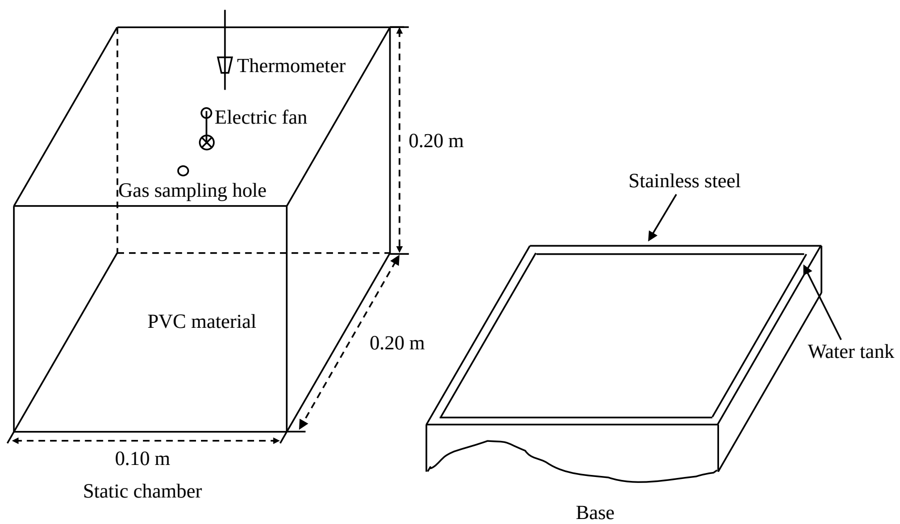

Figure 2. Static chamber.

2.5. Statistical Analysis

The IBM-SPSS statistical package (IBM-SPSS, 19, Chicago, IL, USA) was used to perform analysis of variance (Two-way ANOVA) through a general linear model procedure, and an LSD test was used to assess significant differences ($p < 0.05$) between the means of different treatments. Surfer software (Golden Software Inc., Golden, CO, USA) was used to create the contour maps of soil moisture distribution.

3. Results

3.1. Soil Moisture Distribution

For all SDI treatments, θ varied markedly and non-uniformly in the horizontal and vertical directions (Figure 3, Figure 4, and Figures S1–S4 in Supplemental Data). For each SDI treatment, θ at different distances (0.07, 0.14, and 0.20 m) in a horizontal direction increased gradually with subsequent irrigation events. The soil WFPS decreased initially, then improved with increasing radial distance from 0.07 m to 0.20 m. The WFPS values were particularly increased after the second irrigation at 0.20 m, rather than at 0.07 m or 0.14 m. Across different depths, θ near the emitter buried in the top layer was more significant than in any other soil layer, with downward water movement greater than upward movement at the same horizontal distance from the emitter.

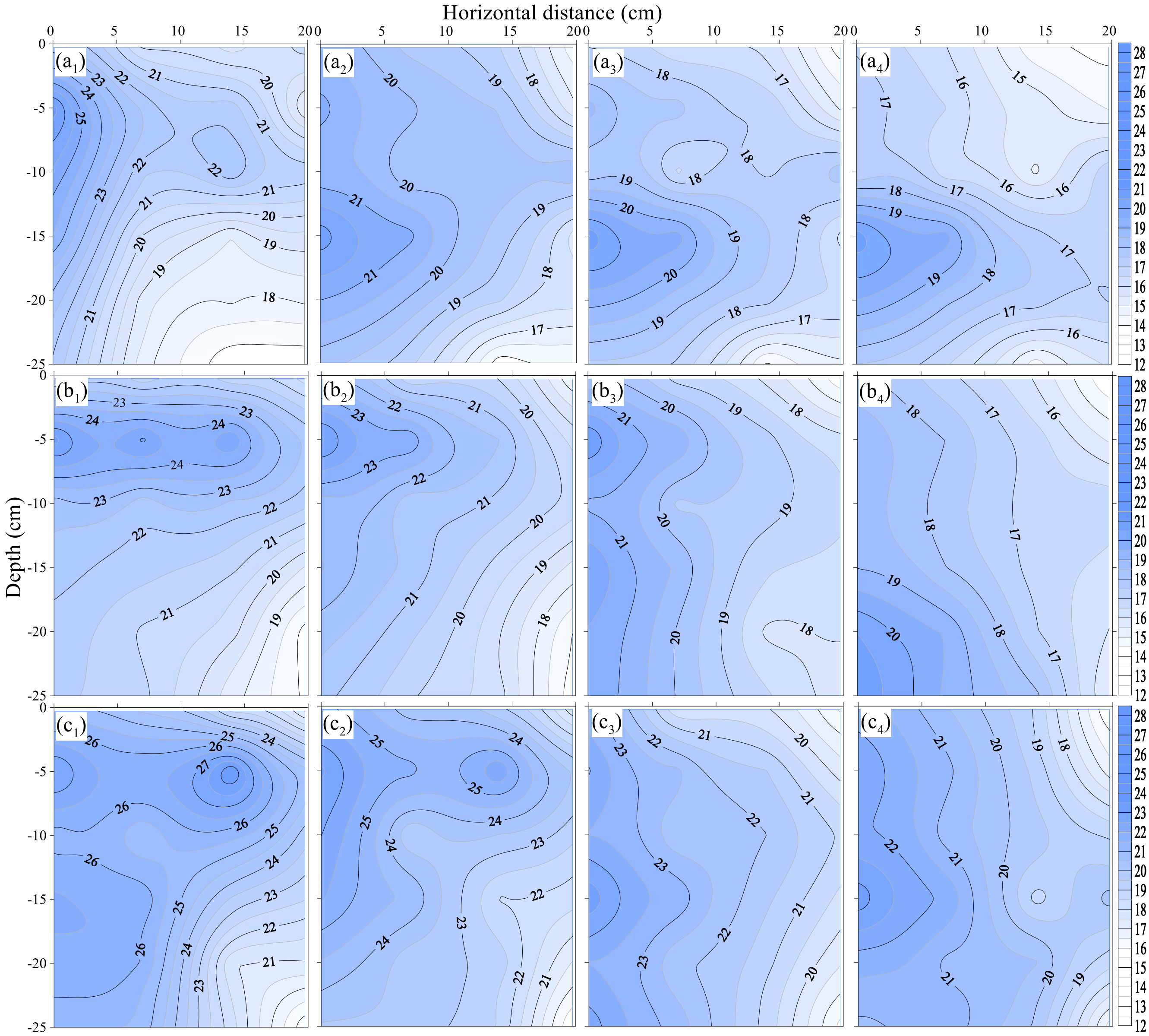

Figure 3. Soil moisture distribution under $SDI_5 + N_{300}$ treatment. Latter **a**, **b**, and **c** represent first, second, and third irrigation events. The subscript numbers 1–4 denote sampling times of soil moisture subsequent to each irrigation.

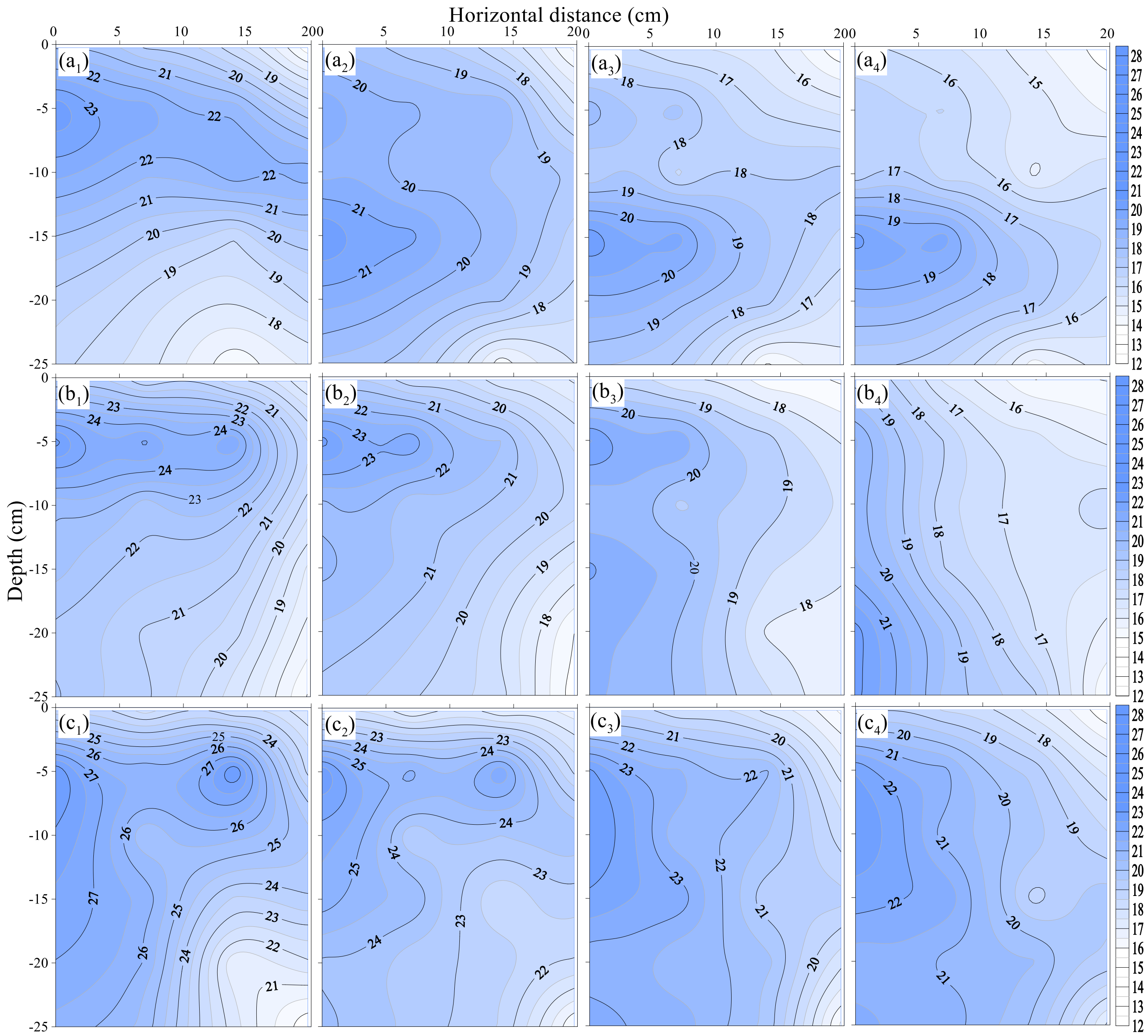

Figure 4. Soil moisture distribution under $SDI_5 + N_{240}$ treatment. Latter **a**, **b**, and **c** represent first, second, and third irrigation events. The subscript numbers 1–4 denote sampling times of soil moisture subsequent to each irrigation.

Taking $SDI_5 + N_{300}$ as an example, the mean (0.05–0.25 m) soil WFPS at 0.07 m ranged from 17.1–20.6%, 18.4–23.0%, and 21.8–27.4% after the first, second, and third irrigation, respectively (Table S1 in Supplemental Data). In contrast, it decreased by 4.2–11.6%, 3.4–9.5%, and 2.5–8.8% at 0.14 m versus (vs.) 0.07 m, and increased by 1.3–2.3%, 9.9–17.9%, and 6.0–13.2% at 0.20 m vs. 0.14 m, respectively. Among the N_{300} treatments, θ showed a similar trend with the emitter at different depths. In contrast, the mean soil WFPS at a depth of 0.05–0.25 m and at distances of 0.07, 0.14, and 0.20 m declined from $SDI_5 + N_{300}$ to $SDI_{15} + N_{300}$. When compared to $SDI_5 + N_{300}$, the mean (0.05–0.25 m) WFPS at 0.07, 0.14, and 0.20 m decreased by 4.5–5.2%, 4.2–5.1%, and 4.3–5.2% for $SDI_{10} + N_{300}$, and 2.4–13.5%, 1.3–12.1%, and 2.8–11.0% for $SDI_{15} + N_{300}$, respectively. Under N_{240} treatments, θ followed a similar pattern to those in N_{300} treatments, whereas the soil WFPS was slightly reduced by 2.8–7.6%, 2.3–10.3%, and 1.8–9.9%, respectively, at 0.07, 0.14, and 0.20 m for

SDI_{10} + N_{240}, and 4.7–11.0%, 2.2–10.2%, and 6.1–9.8% at 0.07, 0.14, and 0.20 m for SDI_{15} + N_{240}, respectively, as compared to SDI_5 + N_{240}.

3.2. NH_4^+-N Concentrations

The average NH_4^+-N concentration under SDI_{15} was significantly greater than that under SDI_5 and SDI_{10} for both the N_{240} and N_{300} levels. Among the N_{300} treatments, the NH_4^+-N concentration showed a similar trend: the mean soil NH_4^+-N in the 0.05–0.25 m depths, across three lateral distances, increased from SDI_5 + N_{300} to SDI_{15} + N_{300}. When compared to SDI_5 + N_{300}, these concentrations increased by 27–371.55%, 25.88–357.05%, and 29.16–347.26% for 0.05, 0.10, and 0.15 m, respectively, under SDI_{10} + N_{300}, and by 46.76–486.06%, 80–498.43%, and 55.52–433.79% for 0.05, 0.10, and 0.15 m, respectively, under SDI_{15} + N_{300}.

For each SDI treatment, the NH_4^+-N concentration at different lateral distances decreased gradually with increased fertigation; moreover, there was a declining trend from one irrigation to the next. Furthermore, NH_4^+-N tended to decline among all treatments as the lateral distance increased: it decreased from 0.07 to 0.14 m, then increased from 0.14 to 0.20 m (Figures 5 and 6; Tables S4–S6 in Supplemental Data). In the vertical direction under SDI_5 + N_{300}, NH_4^+-N decreased as the emitter depth increased, whereas under SDI_{10} + N_{300}, it increased from 0.05 to 0.10 m, then declined at 0.25 m. Meanwhile, under SDI_{15} + N_{300}, it showed an increasing trend from 0.05 to 0.15 m and then decreased (Figure 5). Taking the SDI_5 + N_{300} treatment (Table S4 in Supplemental Data) as an example, after the first three irrigations, let us consider the mean NH_4^+-N from 0.05–0.25 m depths. At 0.07 m, it ranged by 7–23 mg kg^{-1}, 2–15 mg kg^{-1}, and 2–11 mg kg^{-1}; at 0.14 m, it decreased by 19.42–30.02%, 20.96–109.42%, and 11.75–51.12%, respectively; at 0.20 m (vs. 0.14 m), it improved by 57.69–105.46%, 25.08–50.70%, and 4.42–130.15%, respectively. Similar trends were observed for the N_{240} fertilizer level (Figure 5 and Table S4 in Supplemental Data), but no significant differences were found.

3.3. NO_3^--N Concentrations

For all treatments, when considering the average of five soil depths (0.05, 0.10, 0.15, 0.20, and 0.25 m) at each of three lateral points (0.07, 0.14, and 0.20 m) away from the emitter, the NO_3^--N concentrations showed an increasing trend after each fertilization event. Considering the SDI_5 + N_{300} treatment as an example, the mean soil NO_3^--N at a 0.07 m, measured after the first, second, and third irrigation events, ranged from 57–245 mg kg^{-1}, 77-264 mg kg^{-1}, and 83–485 mg kg^{-1}, and these concentrations were 3.36–14.63%, 3.30–19.24%, and 7.72–86.36% greater, respectively, at a 0.14 m distance than at the 0.07 m distance. The soil NO_3^--N after each of the three irrigation events decreased by 25.42–40.20%, 22.26–35.09%, and 28.61–40.13%, respectively, with an increase in the lateral distance from 0.14 m to 0.20 m (Table S7 in Supplemental Data). A similar trend was noted among all N_{300} treatments; namely, soil NO_3^--N concentrations across depths of 0.05 to 0.25 m and at lateral distances of 0.07, 0.14, and 0.20 m declined from SDI_5 + N_{300} to SDI_{15} + N_{300}. After the first, second, and third irrigation events, mean soil NO_3^--N concentrations decreased significantly by 5.19–29.92%, 2.14–19.81%, and 3.31–19.42% for SDI_{10} + N_{300} (Table S8 in supplemental data), and 16.78–41.57%, 11.25–30.08%, and 12.54–30.73% for SDI_{15} + N_{300} (Table S9 in supplemental data), respectively. Soil NO_3^--N levels fluctuated with depth, but differences were insignificant. Generally, NO_3^--N concentrations were greatest at a 0.05 m depth. Concentrations increased with fertilization events and decreased with greater depth. NO_3^--N increased with horizontal distance (Figure 7). The results also demonstrated that soil NO_3^--N under N_{240} treatments followed a similar pattern to those under N_{300} treatments, but their values were lower ($p > 0.05$) (Figure 8).

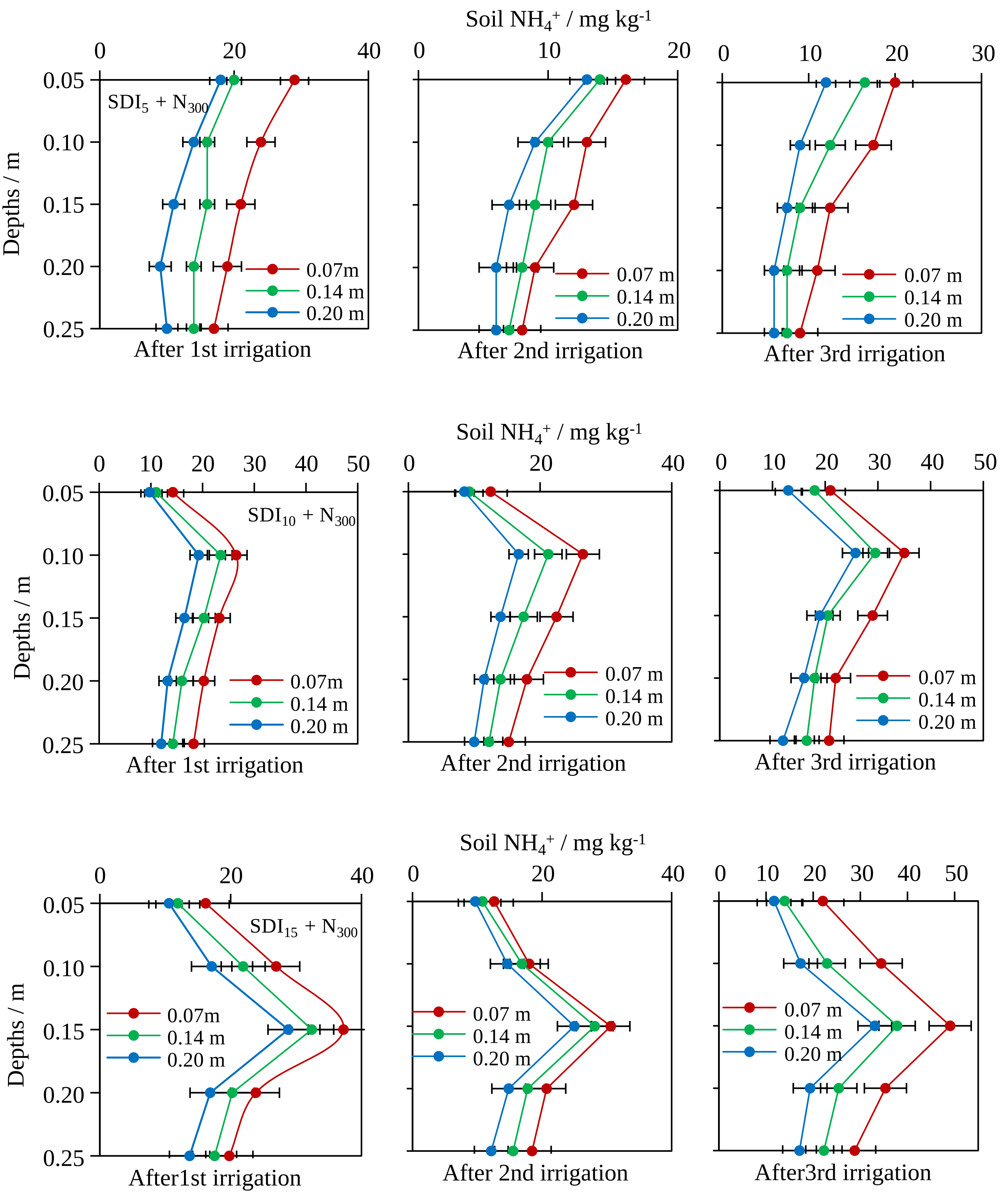

Figure 5. Soil NH_4^+-N after three irrigation events occurring from different emitter depths under the 300 kg N ha^{-1} fertilization rate. Error bars represent standard error.

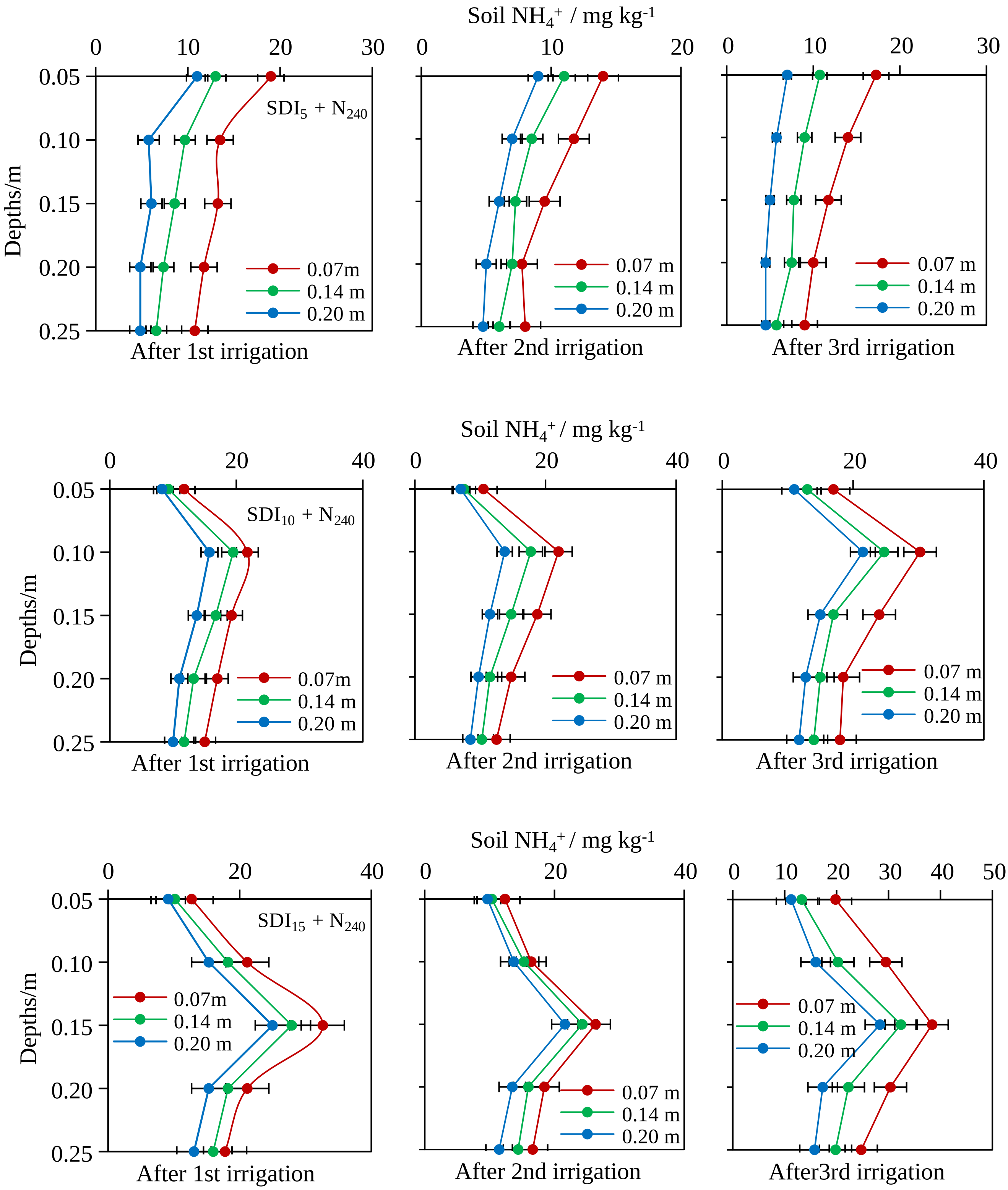

Figure 6. Soil NH_4^+-N after three irrigation events occurring from different emitter depths under the 240 kg N ha^{-1} fertilization rate. Error bars represent standard error.

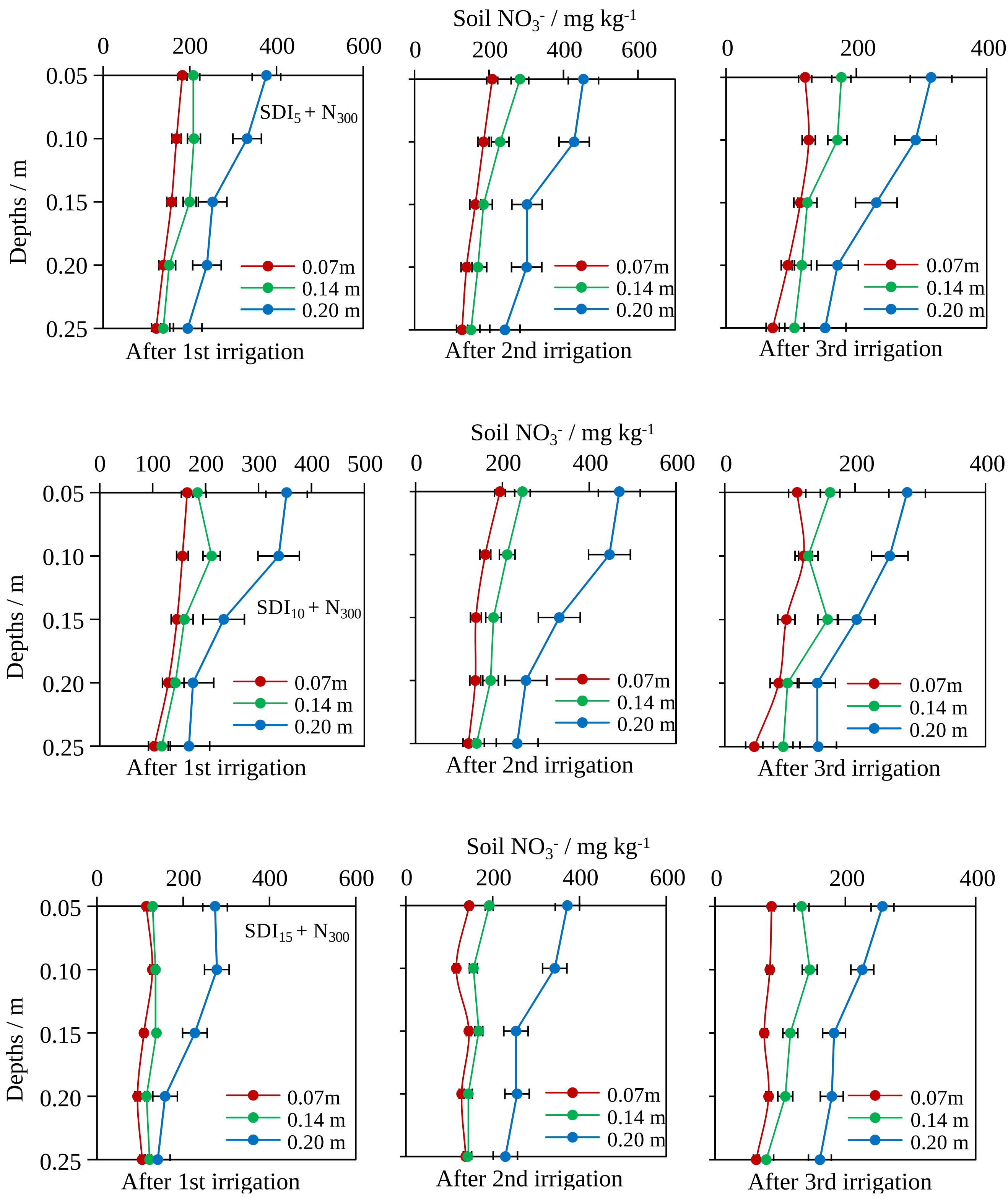

Figure 7. Soil NO_3^--N after three irrigation events occurring from different emitter depths under the 300 kg N ha^{-1} fertilization rate. Error bars represent standard error.

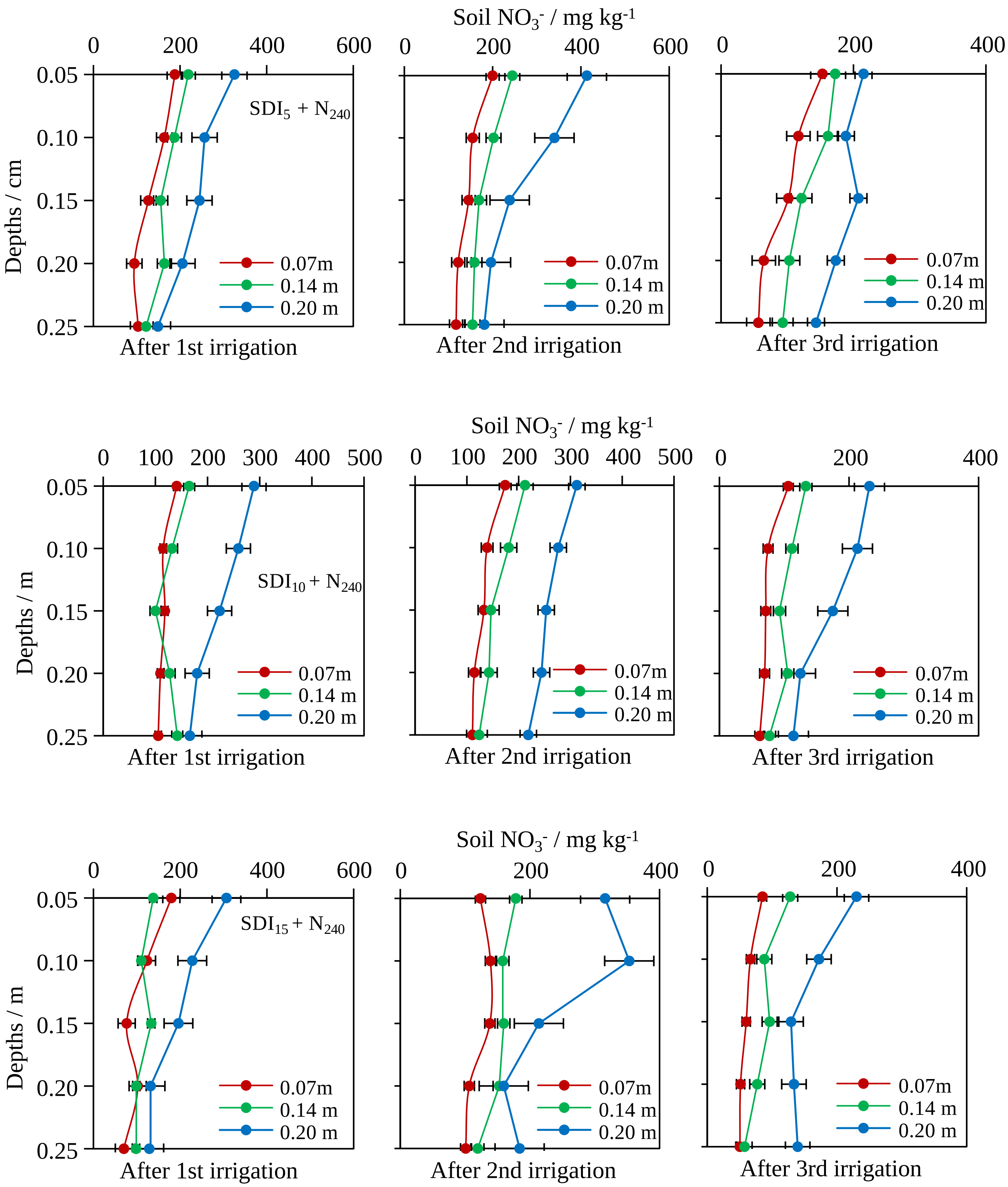

Figure 8. Soil NO_3^--N after each of three irrigation events occurring from different emitter depths under the 240 kg N ha^{-1} fertilization rate. Error bars represent standard error.

3.4. Soil N_2O Emissions

Soil N_2O emissions were influenced by the mineral fertilizer applied and the irrigation system used. Peak soil N_2O emissions occurred in the early hours of the experimental period. The mean peak N_2O flux from five chambers per plot under SDI_5 was

28.95 μg N_2O m^{-2} h^{-1} (Figure 9) and occurred 72 h after the first fertigation event. Fluxes under SDI_5 were greater ($p < 0.05$) than under SDI_{10} and SDI_{15} when the maximum soil WFPS ranged by 20.1–20.6% (Table S1 in Supplemental Data). From 72 h onward (72–360 h), the N_2O fluxes, varying across a range of 4.87–28.95 μg N_2O m^{-2} h^{-1}, declined rapidly with the decrease in θ, particularly when the soil WFPS declined by 17.1–20.6% under the SDI_5 treatment. A similar pattern of average N_2O fluxes occurred after the second and third fertigations, with peak fluxes of 24.82 and 15.53 μg N_2O m^{-2} h^{-1} at WFPS levels of 26.2% and 28.2%, respectively (Table S1 in Supplemental Data). Showing similar patterns to those under SDI_5, N_2O fluxes under SDI_{10} and SDI_{15} treatments resulted in peak N_2O fluxes of 26.60 and 25.60 μg N_2O m^{-2} h^{-1}, respectively (Figure 9) within 72 h of the first watering when the average WFPS was 19.2% or 18.8%, respectively (Tables S2 and S3 in Supplemental Data). Under both N fertilizer rates and over the entire sampling period, the SDI_{15} plots had a lower N_2O flux than the SDI_5 or SDI_{10} plots.

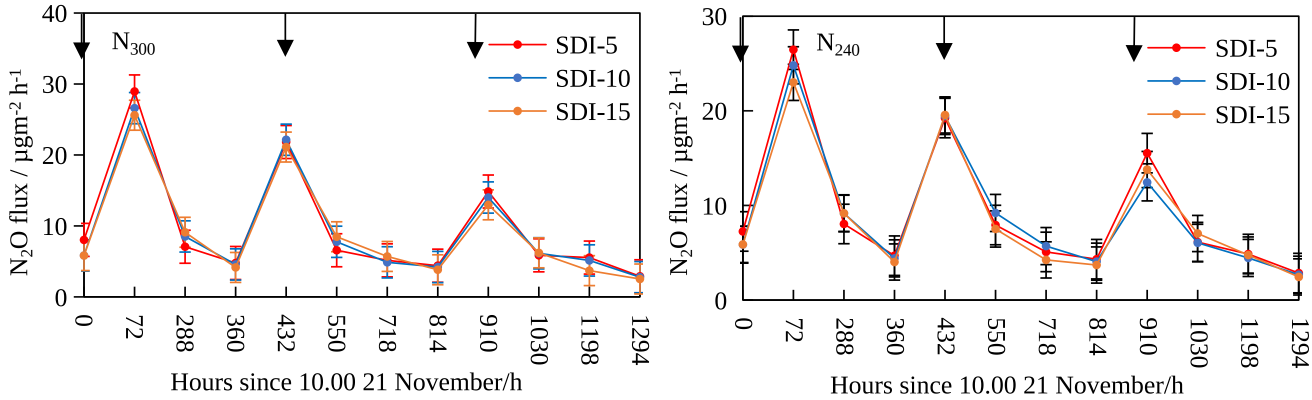

Figure 9. Trend of N_2O flux under different SDI emitter depths over the whole experimental period. Each data point is the mean flux for five chambers replicated three times. Downward arrows represent a water and fertilizer application event. Error bars represent standard error.

Gas fluxes varied with the placement of the chambers relative to the drip irrigation emitter. Within each treatment plot, of the five chambers located at different distances from the emitter, the peak N_2O flux (34.21 μg N_2O m^{-2} h^{-1}) occurred at Chamber 1 (point 1), situated nearest the emitter in a horizontal direction. Under SDI_5 + N_{300}, this first peak occurred within 72 h after the first irrigation. The N_2O flux decreased gradually until another peak (28.40 μg N_2O m^{-2} h^{-1}) occurred at 432 h after the first watering event, and a third peak (18.96 μg N_2O m^{-2} h^{-1}) occurred after 910 h (Figure 10). Under SDI_5 + N_{240}, peak N_2O fluxes of 30.12, 23.68, and 18.93 μg N_2O m^{-2} h^{-1} occurred after 72, 432, and 910 h, respectively. As shown in Figure 10, for the other sampling points, either under N_{300} or N_{240}, the trend was similar in that fluxes increased initially after each watering event then decreased gradually until the following irrigation event. In general, the obvious emission peaks were observed 1–3 days after each irrigation.

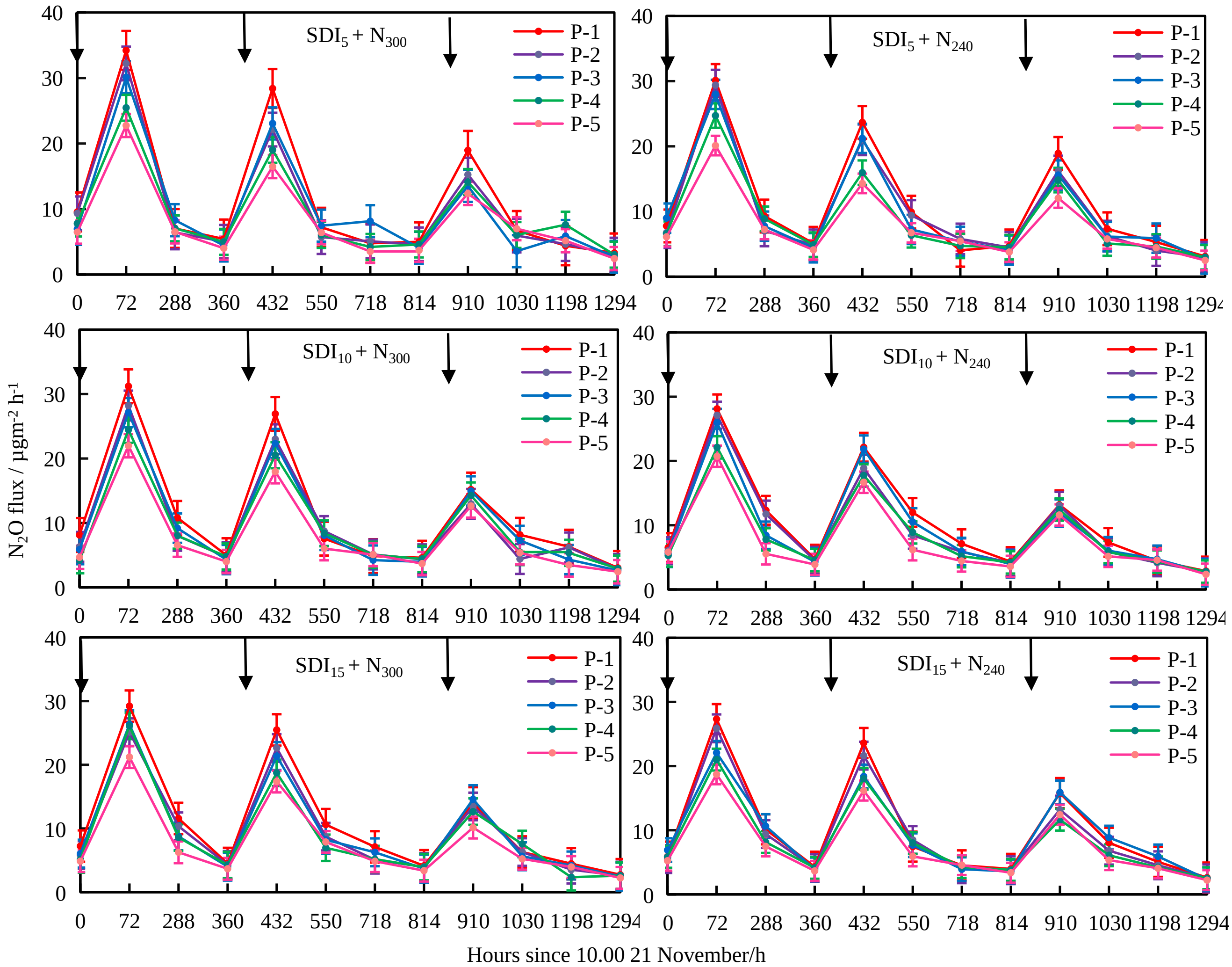

Figure 10. Trend of N_2O flux under different SDI emitter depths over the entire experimental period. P-1, P-2, P-3, P-4, and P-5 represent chambers 1–5. Arrows represent water and fertilizer application events. Error bars represent standard error.

3.5. Relationship between N_2O Emissions and Soil WFPS, NH_4^+-N, and NO_3^--N

Pearson correlation analysis showed non-significant positive correlation coefficients (R^2) after the first, second, and third fertigations for N_2O fluxes and soil WFPS. At all five sampling points, the highest R^2 values occurred at a depth of 0.05 m and a lateral distance of 0.07 m. At a lateral distance of 0.14 m, the maximum R^2 was observed at a 0.15 m depth, while at a lateral distance of 0.20 m, the highest R^2 value was at a 0.10 m depth (Table 1 and Tables S10 and S11 in Supplemental Data). The N_2O flux increased with WFPS while NH_4^+-N was positively correlated with N_2O ($p < 0.05$, Tables S12–S14 in Supplemental Data), whereas a negative relationship was observed with NO_3^--N ($p < 0.05$, Tables S15–S17 in Supplemental Data).

Table 1. Pearson correlation coefficients (R^2) between N_2O emissions and soil moisture at different depths under the SDI_5 irrigation treatment.

Treatment	Horizontal Distance (m)	Depths (cm)	Point 1	Point 2	Point 3	Point 4	Point 5
$SDI_5 + N_{300}$	0.07 m	5	**0.0896**	**0.0523**	**0.0406**	**0.0784**	**0.0948**
		10	0.0681	0.0429	0.0237	0.0689	0.0759
		15	0.0366	0.0215	0.0107	0.0507	0.0614
		20	0.0308	0.0145	0.0058	0.0373	0.0447
		25	0.0048	0.0001	0.0040	0.0074	0.0089
	0.14 m	5	0.1436	0.0975	0.0691	0.1374	0.1582
		10	0.0893	0.0611	0.0383	0.0893	0.1017
		15	**0.1834**	**0.1396**	**0.1125**	**0.1980**	**0.2223**
		20	0.0148	0.0073	0.0013	0.0268	0.0350
		25	0.0116	0.0267	0.0348	0.0102	0.0072
	0.20 m	5	0.0916	0.0449	0.0437	0.0757	0.0865
		10	**0.1143**	**0.0668**	**0.0520**	**0.1030**	**0.1170**
		15	0.0065	0.0001	0.0007	0.0058	0.0077
		20	0.0096	0.0008	0.0000	0.0100	0.0122
		25	0.0197	0.0025	0.0054	0.0136	0.0146
$SDI_5 + N_{240}$	0.07 m	5	**0.1076**	**0.0776**	**0.0906**	**0.0457**	**0.0813**
		10	0.0819	0.0565	0.0715	0.0377	0.0597
		15	0.0674	0.0403	0.0438	0.0432	0.0526
		20	0.0568	0.0346	0.0321	0.0337	0.0401
		25	0.0118	0.0039	0.0043	0.0014	0.0046
	0.14 m	5	0.1719	0.1259	0.1455	0.1015	0.1393
		10	0.1087	0.0755	0.0990	0.0604	0.0890
		15	**0.2330**	**0.1800**	**0.1971**	**0.1646**	**0.2032**
		20	0.0248	0.0108	0.0160	0.0062	0.0135
		25	0.0071	0.0132	0.0139	0.0316	0.0156
	0.20 m	5	0.1090	0.0786	0.0816	0.0417	0.0738
		10	**0.1384**	**0.0980**	**0.1083**	**0.0668**	**0.0979**
		15	0.0114	0.0029	0.0044	0.0000	0.0023
		20	0.0158	0.0058	0.0073	0.0007	0.0051
		25	0.0236	0.0136	0.0133	0.0008	0.0092

Note: Values in bold are the maximum correlation among five depths at each point.

3.6. Chinese Cabbage Yield

The Chinese cabbage yield was greatest for $SDI_{15} + N_{300}$, followed by the $SDI_{10} + N_{300}$ and $SDI_5 + N_{300}$ treatments. Compared to the yield under $SDI_5 + N_{300}$, the yields under $SDI_{10} + N_{300}$ and $SDI_{15} + N_{300}$ were 4.33% and 41.73% greater (Table 2). A similar pattern was found under the N_{240} treatments, with the following order: $SDI_{15} + N_{240} > SDI_{10} + N_{240} > SDI_5 + N_{240}$. Compared with $SDI_5 + N_{240}$, the crop yield significantly increased by 16.9% and 57.92% for $SDI_{10} + N_{240}$ and $SDI_{15} + N_{240}$, respectively. The emitter depth and N level significantly affected the crop yield, but their interaction effect was insignificant (Table 2).

Table 2. Effect of different SDI emitter depths and fertilizer management on Chinese cabbage yield.

Treatment	Yield kg m^{-2}
$SI + N_{300}$	2.54 ± 0.11 ^{C}
$SI + N_{240}$	1.83 ± 0.08 ^{E}
$DI + N_{300}$	2.65 ± 0.11 ^{BC}
$DI + N_{240}$	2.14 ± 0.09 ^{D}
$SDI_5 + N_{300}$	3.60 ± 0.15 ^{A}
$SDI_5 + N_{240}$	2.89 ± 0.12 ^{B}
I	*
N	*
I × N	ns

Note: SDI_5, SDI_{10}, and SDI_{15} represent subsurface drip irrigation with drippers buried at 5, 10, and 15 cm below the soil surface, respectively. I and N represent irrigation and nitrogen, respectively. Values of the column followed with different uppercase letters are significantly different at $p < 0.05$ according to the LSD test. * and ns denote significance and non-significance at the p-level, respectively.

4. Discussion

4.1. Effect of Soil Moisture on N_2O Emissions

Irrigation practices directly affect θ dynamics, leading to greater GHG emissions [20]. As one of the main factors affecting soil N_2O emissions after precipitation or irrigation, θ remains high for a short period and declines rapidly in the topsoil layer according to the climate conditions such as temperature and solar radiation [21–23]. Greater θ increases anaerobic microsites and promotes N_2O emission via denitrification [24]. Continuous efforts are required to improve the quantification of N_2O emissions from different agricultural practices and N-fertilized crops [25]. In the current study, under either N_{240} or N_{300} nitrogen fertilization levels, the highest θ occurred under SDI_5. The maximum θ value was observed immediately after each irrigation event and declined slowly until the next. The mean soil WFPS varied from 14.2 to 28.2% during the entire observation period, which was slightly lower than the values reported by previous studies. For example, Hou et al. [6] reported that peak N_2O emissions were generally observed when the WFPS was in the range of 45–90%. Low θ may affect the transfer of NH_4^+-N by microorganisms, resulting in low N_2O emissions. Our findings concur with those of [4]. Sanchez-Martin et al. [14] noted that the biggest pulses of N_2O emissions occurred after the first irrigation. Indeed, the application of water to dry soil results in the activation of microorganisms and a rise in N_2O emissions [26]. In the present study, N_2O produced under the SDI_{15} treatment was less than that generated under the SDI_5 and SDI_{10} treatments ($p < 0.05$). This might be attributable to N_2O produced under SDI_{15} perhaps not reaching the atmosphere or being restricted because of N_2O consumption reactions in the upper soil layers [27]. A study by Rychel et al. [28], supported in its general conclusions by the work of Xu et al. [4], found that N_2O emissions under a shallow fertilizer placement (0.07 m) treatment were generally greater than those occurring under a deep fertilizer placement (0.20 m). The present results indicated that after the first watering event, the WFPS distanced 0.07 m laterally from an emitter was higher than at lateral distances of 0.14 or 0.20 m. This was attributable to the water distribution and the distance from the emitter. In contrast, after the second and third irrigation events, the WFPS at 0.20 m > 0.07 m > 0.14 m, possibly because some overlap in watering might have occurred. We agree with the observations of Li et al. [29] and Sanchez-Martin et al. [14], who concluded that the soil volume remains dry after the first irrigation, but after each subsequent irrigation event, the wetting front advances slightly. Our findings were also supported by Kuang et al. [5], who stated that the WFPS of areas away from drip tape was low.

Vertical θ distribution characteristics under different irrigation regimes will change N_2O emission patterns [4]. Within each treatment, we found that the mean WFPS at a depth of 0.05 m tended to be greater than at greater depths but that any differences were not significant. The θ decreased with an increase in the lateral distance from the emitter, and the θ distribution shifted quickly after irrigation as water could move easily through the soil, then slow down gradually (Figures 3 and 4) due to dry soil conditions. Observing the five different chambers sampled for a given treatment, N_2O flux in a chamber (P1) near the emitter was greater than at other more distal points. This could have been due to higher θ proximal to the emitter, which favored the proliferation of microorganisms involved in the nitrification and denitrification processes. Our findings are consistent with Schaufler et al. [24], who reported that N_2O emissions declined when the θ was low and limited microbial activity. According to the Pearson correlation analysis, soil WFPS was positively correlated to N_2O emissions among all SDI treatments and for both N fertilization treatment (N_{240} and N_{300}) levels (Table 1 and Tables S10 and S11 in Supplemental Data). Weslien et al. [30] also noted that N_2O fluxes were positively correlated to the WFPS.

4.2. Effect of Soil NH_4^+-N Distribution on N_2O Emissions

N_2O is derived from nitrification and denitrification processes occurring in the soil, which rely on the availability of NH_4^+-N and NO_3^--N, respectively, and on θ, in addition to other factors [31,32]. The soil NH_4^+-N concentration after the first irrigation event rapidly decreased, and values were less than 7 mg NH_4^+-N kg^{-1} in subsequent days [33]. Our findings showed that NH_4^+-N was significantly greater under SDI_5 than SDI_{10}, while for both, it was greater than under SDI_{15}. Within each treatment, the maximum NH_4^+-N concentration occurred after each irrigation event, then decreased until the next irrigation. Among the five vertical sampling depths, NH_4^+-N in the upper soil layer (0.05 m) was higher than in deeper soil layers. Similar to the work of Li et al. [29], we found a high NH_4^+-N concentration close to the point source (about 0.025–0.075 m from the source).

Moreover, correlation analysis indicated that NH_4^+-N had a positive and significant relationship with N_2O emissions. For instance, for $SDI_5 + N_{300}$ at a 0.07 m lateral distance, a significant correlation was noted at depths of 0.05 m, 0.20 m, and 0.25 m, with the maximum R^2 values occurring at a 0.05 m depth. For a 0.14 m horizontal distance, NH_4^+-N significantly correlated with N_2O at 0.05 m and 0.25 m depths, with the maximum R^2 values registered at the latter depth. Furthermore, some correlations were found at a 0.20 m horizontal distance, with the R^2 values highest in the upper layers (Table S12 in Supplemental Data).

4.3. Effect of Soil NO_3^--N Distribution on N_2O Emissions

Application of nitrogen with SDI places NO_3^--N below the soil surface and within the root zone, facilitating crop uptake [34]. In another study, the NO_3^--N concentration increased significantly as the radial distance from the emitter exceeded 0.20 m [29]. In the current study, across all treatments, an increasing trend in soil NO_3^--N occurred after each irrigation/fertilization event until the following such event (sampling times were between fertigation events). We speculate that due to decreasing θ, and because NO_3^--N is very soluble in water, it remains in the soil rather than being taken up by the plant or converted into emissions. The present findings demonstrate that for all treatments, the average NO_3^--N concentrations at a 0.20 m lateral distance from the emitter were significantly greater ($p < 0.05$) than at other distances, which may be due to the crop roots being unable to reach this point to take up NO_3^--N. While no significant difference in NO_3^--N was found between the N_{240} and N_{300} fertilization rates, NO_3^--N levels tended to be slightly higher at the N_{300} level, perhaps indicating that an increase in fertilization rate will increase the N_2O emission rate. These findings confirmed the observations of Hoben et al. [35], who reported that the N_2O emissions increase with an increasing N fertilization rate. The results also concur with those of Kong et al. [36], who observed in an apple orchard that the cumulative production of N_2O tended to increase with increasing N doses. In the present study, correlation analysis indicated that NO_3^--N concentrations were negatively correlated to soil N_2O emission ($p < 0.05$). Taking $SDI_5 + N_{300}$ (Table S15) as an example, NO_3^--N, at a lateral distance of 0.07 m, was mainly concentrated in the 0.10–0.25 m soil depth, with the maximum correlations coefficient generally occurring at a 0.15 m depth. For the 0.14 m horizontal distance, the NO_3^--N concentration was significantly correlated to N_2O at depths of 0.05, 0.15, 0.20, and 0.25 m, with a maximum R^2 at 0.20 m. At a 0.20 m horizontal distance, significant correlations were observed at a depth of 0.25 m (Table S15 in Supplemental Data). Furthermore, under $SDI_5 + N_{240}$, for both the 0.07 m and 0.14 m horizontal distances, significant correlations occurred at depths from 0.10–0.25 m. At a 0.20 m horizontal distance, significant correlations were only observed at a 0.15 m depth (Table S15 in Supplemental Data). A study by Weslien et al. [30] also reported that N_2O fluxes were negatively correlated to the soil NO_3^--N concentrations. According to the results, N_2O emissions were not regulated by NO_3^--N availability alone, but other factors were involved. As N_2O emissions in our study were low, we speculate that low soil aeration and temperature during the winter season might have reduced microbial activity. Our findings are supported by Kuang et al. [5], who found that low N_2O emissions are likely associated with the cool overnight air and soil temperature under arid conditions. Beyond this, another reason for low N_2O emissions could be the lack of NO_3^--N and water uptake by the crop.

4.4. Crop Yield

Under the SDI method, greater irrigation water use efficiency and higher yields were recorded with lesser water applications: the yield and water use efficiency for SDI emitters at a 0.15 m depth were significantly higher than at other depths [37]. In the SDI_5 and SDI_{10} treatments, the soil moisture was mainly concentrated in the shallow soil layers (5~10 cm). Under the evaporation and transpiration processes, the soil moisture and nitrogen of these parts of the soil layers were more prone to loss into the atmospheric system in the form of water vapor, resulting in a decrease in the amount of water supposedly absorbed and utilized by the plant. At the same time, the reduction of soil moisture also led to an increase in soil temperature, which is another crucial factor affecting crop growth. In contrast, under the condition of SDI_{15}, soil water was mainly concentrated in the deeper soil layers, and its evaporation was limited, resulting in the absorption of more water stored in the soil. In addition, with the growth of the crop, the central root zone was also increasing. Chinese cabbage's primary root water absorption zone is 5~10 cm, and a more reasonable water distribution and higher water content in the root zone promote crop yield improvement. These results concur with Singh and Rajput [38], who found that the yield was significantly greater when emitters were placed at depths of 0.10 m and 0.15 m below the soil surface.

4.5. Limitations of Subsurface Drip Irrigation and Future Work

The flow rate of the dripper in this study was 3 L h^{-1}, but with an increase of soil moisture near the drippers and extension of the irrigation pipes, the drippers' flow rate should be gradually reduced. This problem can be estimated by the water flow meters installed at different drippers, and we believe this is also an interesting research direction. However, in the current study, we focused on the effects of the same irrigation amount on soil water and nitrogen dynamics and soil N_2O emissions under the condition of different dripper burial depths of SDI. In future research, we will conduct experiments on the impacts of dripper flow on soil water, nitrogen, and soil N_2O emissions. We will also study the effects of different irrigation regimes on soil water and nitrogen dynamics and N_2O emissions under different burial depths of SDI based on changes in soil moisture.

5. Conclusions

In this paper, we have presented the findings of our investigation into N_2O emissions under SDI with emitters at different depths and N fertilization rates. Compared to the SDI_5 and SDI_{10} treatments, SDI_{15} reduced the N_2O emissions and increased the Chinese cabbage yield. Within each treatment, the placement of the chamber affected the N_2O emissions, with a chamber 0.05 m away from the emitter contributing higher emissions than the four laterally farther away. Emissions of N_2O increased with WFPS and NH_4^+-N concentrations but declined with an increase in soil NO_3^--N. The present study showed the N_{300} fertilization rate to result in slightly greater WFPS, NH_4^+-N, NO_3^--N, and N_2O emission levels than N_{240}; however, these differences were not significant. The extent of N_2O emissions was positively correlated to WFPS and NH_4^+-N but negatively to NO_3^--N. Our results suggest that to reduce N_2O emissions and enhance Chinese cabbage yield, a combination of SDI techniques with emitters buried at a 0.15 m depth and N fertilizers should be considered. However, understanding horizontal and vertical water distribution dynamics is a strategic underpinning of agriculture production because it saves water, mitigates emissions, and enhances the yield. Moreover, increasing the fertilizer placement depth can improve agricultural practices and mitigate GHG emissions. More studies are necessary to thoroughly understand the influence of irrigation and N management strategies, and their vertical and horizontal distribution, to mitigate N_2O emissions from agricultural soils.

Supplementary Materials: The following are available online at https://www.mdpi.com/article/10.3390/agronomy12030745/s1, Figure S1: Soil moisture distribution under SDI10+N300 treatment. letters a, b, and c represent first, second, and third irrigation events. The subscript numbers 1, 2, 3, and 4 denote sampling times of soil moisture subsequent to each irrigation; Figure S2: Soil moisture distribution under SDI15+N300 treatment. letters a, b, and c represent first, second, and third irrigation events. The subscript numbers 1, 2, 3, and 4 denote sampling times of soil moisture within each irrigation; Figure S3: Soil moisture distribution under SDI_{10} + N_{240} treatment. Letters a, b, and c represent first, second, and third irrigation events. The subscript numbers 1, 2, 3, and 4 denote sampling times of soil moisture subsequent to each irrigation; Figure S4: Soil moisture distribution under SDI_{15} + N_{240} treatment. letters a, b, and c represent first, second, and third irrigation events. The subscript numbers 1, 2, 3, and 4 denote sampling times of soil moisture within each irrigation, Table S1: Soil average ± standard deviation of WFPS% for SD15 treatments; Table S2: Soil average ± standard deviation of WFPS% for SD110 treatments; Table S3: Soil average ± standard deviation of WFPS% for SD115 treatments; Table S4: Soil average ± standard deviation of NH_4^+-N mg kg^{-1} under SD15 treatments; Table S5: Soil average ± standard deviation of NH_4^+-N mg kg^{-1} under SD110 treatments; Table S6: Soil average ± standard deviation of NH_4^+-N mg kg^{-1} under SD115 treatments; Table S7: Soil average ± standard deviation of NO_3^--N mg kg^{-1} under SD15 treatments; Table S8: Soil average ± standard deviation of NO_3^--N mg kg^{-1} under SD110 treatments; Table S9: Soil average ± standard deviation of NO_3^--N mg kg^{-1} under SD115 treatments; Table S10: Correlations (R2) between N_2O emissions and soil moisture at different depths under SDI10; Table S11: Correlations (R2) between N_2O emissions and soil moisture at different depths under SDI15; Table S12: Correlations (R2) between N_2O emissions and soil NH_4^+-N at different depths under SDI5; Table S13: Correlations (R2) between N_2O emissions and soil NH_4^+-N at different depths under SDI10; Table S14: Correlations (R2) between N_2O emissions and soil NH_4^+-N at different depths under SDI15; Table S15: Correlations (R2) between N_2O emissions and soil NO_3^- at different depths under SDI5; Table S16: Correlations (R2) between N_2O emissions and soil NO_3^- at different depths under SDI10; Table S17: Correlations (R2) between N_2O emissions and soil NO_3^- at different depths under SDI15.

Author Contributions: Conceptualization, A.A.A.H. and J.X.; methodology, A.A.A.H., L.W. and Q.W.; statistical analysis, A.A.A.H., Q.W. and H.S.; writing—original draft preparation, A.A.A.H.; writing—review and editing, Y.A.H., A.A.A.H. and Y.L. All authors have read and agreed to the published version of the manuscript.

Funding: This research was funded by Fundamental Research Funds for the Central Universities (B200201004) and the National Natural Science Foundation of China (51809077, 51879075).

Institutional Review Board Statement: Not applicable.

Informed Consent Statement: Not applicable.

Data Availability Statement: Not applicable.

Conflicts of Interest: The authors declare no conflict of interest.

References

1. Gao, S.; Hendratna, A.; Cai, Z.; Duan, Y.; Qin, R.; Rebecca, T.-C. Subsurface Drip Irrigation Reduced Nitrous Oxide Emissions in a Pomegranate Orchard. *Int. J. Environ. Sci. Dev.* **2019**, *10*, 79–85. [CrossRef]
2. Harwood, J.E.; Huyser, D.J. Automated Analysis of Ammonia in Water. *Water Res.* **1970**, *4*, 695–704. [CrossRef]
3. Syakila, A.; Kroeze, C. The Global Nitrous Oxide Budget Revisited. *Greenh. Gas Meas. Manag.* **2011**, *1*, 17–26. [CrossRef]
4. Xu, J.; Wei, Q.; Yang, S.; Wang, Y.; Lv, Y. Diurnal Pattern of Nitrous Oxide Emissions from Soils under Different Vertical Moisture Distribution Conditions. *Chil. J. Agric. Res.* **2016**, *76*, 84–92. [CrossRef]
5. Kuang, W.; Gao, X.; Gui, D.; Tenuta, M.; Flaten, D.N.; Yin, M.; Zeng, F. Effects of Fertilizer and Irrigation Management on Nitrous Oxide Emission from Cotton Fields in an Extremely Arid Region of Northwestern China. *Field Crops Res.* **2018**, *229*, 17–26. [CrossRef]
6. Hou, H.; Yang, S.; Wang, F.; Li, D.; Xu, J. Controlled Irrigation Mitigates the Annual Integrative Global Warming Potential of Methane and Nitrous Oxide from the Rice–Winter Wheat Rotation Systems in Southeast China. *Ecol. Eng.* **2016**, *86*, 239–246. [CrossRef]
7. Wu, J.; Guo, W.; Feng, J.; Li, L.; Yang, H.; Wang, X.; Bian, X. Greenhouse Gas Emissions from Cotton Field under Different Irrigation Methods and Fertilization Regimes in Arid Northwestern China. *Sci. World J.* **2014**, *2014*, 407832. [CrossRef] [PubMed]

8. Ye, X.H.; Han, B.; Li, W.; Zhang, X.C.; Zhang, Y.L.; Lin, X.G.; Zou, H.T. Effects of Different Irrigation Methods on Nitrous Oxide Emissions and Ammonia Oxidizers Microorganisms in Greenhouse Tomato Fields. *Agric. Water Manag.* **2018**, *203*, 115–123. [CrossRef]
9. Edwards, K.P.; Madramootoo, C.A.; Whalen, J.K.; Adamchuk, V.I.; Mat Su, A.S.; Benslim, H. Nitrous Oxide and Carbon Dioxide Emissions from Surface and Subsurface Drip Irrigated Tomato Fields. *Can. J. Soil Sci.* **2018**, *98*, 389–398. [CrossRef]
10. Delang, C.O. Causes and Distribution of Soil Pollution in China. *Environ. Socio-Econ. Stud.* **2017**, *5*, 1–17. [CrossRef]
11. Alhaj Hamoud, Y.; Guo, X.; Wang, Z.; Shaghaleh, H.; Chen, S.; Hassan, A.; Bakour, A. Effects of Irrigation Regime and Soil Clay Content and Their Interaction on the Biological Yield, Nitrogen Uptake and Nitrogen-Use Efficiency of Rice Grown in Southern China. *Agric. Water Manag.* **2019**, *213*, 934–946. [CrossRef]
12. Alhaj Hamoud, Y.; Shaghaleh, H.; Sheteiwy, M.; Guo, X.; Elshaikh, N.A.; Ullah Khan, N.; Oumarou, A.; Rahim, S.F. Impact of Alternative Wetting and Soil Drying and Soil Clay Content on the Morphological and Physiological Traits of Rice Roots and Their Relationships to Yield and Nutrient Use-Efficiency. *Agric. Water Manag.* **2019**, *223*, 105706. [CrossRef]
13. Kumar Jha, S.; Ramatshaba, T.S.; Wang, G.; Liang, Y.; Liu, H.; Gao, Y.; Duan, A. Response of Growth, Yield and Water Use Efficiency of Winter Wheat to Different Irrigation Methods and Scheduling in North China Plain. *Agric. Water Manag.* **2019**, *217*, 292–302. [CrossRef]
14. Sánchez-Martín, L.; Vallejo, A.; Dick, J.; Skiba, U.M. The Influence of Soluble Carbon and Fertilizer Nitrogen on Nitric Oxide and Nitrous Oxide Emissions from Two Contrasting Agricultural Soils. *Soil Biol. Biochem.* **2008**, *40*, 142–151. [CrossRef]
15. Maris, S.C.; Teira-Esmatges, M.R.; Arbonés, A.; Rufat, J. Effect of Irrigation, Nitrogen Application, and a Nitrification Inhibitor on Nitrous Oxide, Carbon Dioxide and Methane Emissions from an Olive (*Olea europaea* L.) Orchard. *Sci. Total Environ.* **2015**, *538*, 966–978. [CrossRef] [PubMed]
16. Wei, Q.; Xu, J.; Li, Y.; Liao, L.; Liu, B.; Jin, G.; Hameed, F. Reducing Surface Wetting Proportion of Soils Irrigated by Subsurface Drip Irrigation Can Mitigate Soil N_2O Emission. *Int. J. Environ. Res. Public Health* **2018**, *15*, 2747. [CrossRef]
17. Wei, Q.; Xu, J.; Yang, S.; Qi, Z.; Wang, Y.; Liao, L. Partial Wetting Irrigation Resulted in Non-Uniformly Low Nitrous Oxide Emissions from Soil. *Atmos. Environ.* **2017**, *161*, 200–209. [CrossRef]
18. Hamad, A.A.A.; Xu, J.; Wei, Q.; Hamoud, Y.A.; Shaghaleh, H.; Wang, K.; Hameed, F.; Xu, L. Effect of Different Irrigation and Nitrogen Management Options on Growth, Yield and Water Use Efficiency of Chinese Cabbage in Greenhouse Cultivation. *Pak. J. Agric. Sci.* **2021**, *58*, 341–356.
19. Ning, D.; Qin, A.; Duan, A.; Xiao, J.; Zhang, J.; Liu, Z.; Liu, Z.; Zhao, B.; Liu, Z. Deficit Irrigation Combined with Reduced N-Fertilizer Rate Can Mitigate the High Nitrous Oxide Emissions from Chinese Drip-Fertigated Maize Field. *Glob. Ecol. Conserv.* **2019**, *20*, e00803. [CrossRef]
20. Tian, D.; Zhang, Y.; Mu, Y.; Zhou, Y.; Zhang, C.; Liu, J. The Effect of Drip Irrigation and Drip Fertigation on N_2O and NO Emissions, Water Saving and Grain Yields in a Maize Field in the North China Plain. *Sci. Total Environ.* **2017**, *575*, 1034–1040. [CrossRef]
21. El-Shafie, A.F.; Osama, M.A.; Hussein, M.M.; El-Gindy, A.M.; Ragab, R. Predicting Soil Moisture Distribution, Dry Matter, Water Productivity and Potato Yield under a Modified gated Pipe Irrigation System: SALTMED Model Application Using Field Experimental Data. *Agric. Water Manag.* **2017**, *184*, 221–233. [CrossRef]
22. Gao, J.; Yan, Y.; Hou, X.; Liu, X.; Zhang, Y.; Huang, S.; Wang, P. Vertical Distribution and Seasonal Variation of Soil Moisture after Drip-Irrigation Affects Greenhouse Gas Emissions and Maize Production during the Growth Season. *Sci. Total Environ.* **2021**, *763*, 142965. [CrossRef] [PubMed]
23. Reyes-Cabrera, J.; Zotarelli, L.; Dukes, M.D.; Rowland, D.L.; Sargent, S.A. Soil Moisture Distribution under Drip Irrigation and Seepage for Potato Production. *Agric. Water Manag.* **2016**, *169*, 183–192. [CrossRef]
24. Schaufler, G.; Kitzler, B.; Schindlbacher, A.; Skiba, U.; Sutton, M.A.; Zechmeister-Boltenstern, S. Greenhouse Gas Emissions from European Soils under Different Land Use: Effects of Soil Moisture and Temperature. *Eur. J. Soil Sci.* **2010**, *61*, 683–696. [CrossRef]
25. Meng, Y.; Wang, J.J.; Wei, Z.; Dodla, S.K.; Fultz, L.M.; Gaston, L.A.; Xiao, R.; Park, J.H.; Scaglia, G. Nitrification Inhibitors Reduce Nitrogen Losses and Improve Soil Health in a Subtropical Pastureland. *Geoderma* **2021**, *388*, 114947. [CrossRef]
26. Dick, J.; Skiba, U.; Wilson, J. The Effect of Rainfall on NO and N_2O Emissions from Ugandan Agroforest Soils. *Phyton* **2001**, *41*, 73–80.
27. Li, Y.; Gao, X.; Tenuta, M.; Gui, D.; Li, X.; Xue, W.; Zeng, F. Enhanced Efficiency Nitrogen Fertilizers Were Not Effective in Reducing N_2O Emissions from a Drip-Irrigated Cotton Field in Arid Region of Northwestern China. *Sci. Total Environ.* **2020**, *748*, 141543. [CrossRef]
28. Rychel, K.; Meurer, K.H.E.; Börjesson, G.; Strömgren, M.; Getahun, G.T.; Kirchmann, H.; Kätterer, T. Deep N Fertilizer Placement Mitigated N_2O Emissions in a Swedish Field Trial with Cereals. *Nutr. Cycl. Agroecosystems* **2020**, *118*, 133–148. [CrossRef]
29. Li, J.; Zhang, J.; Ren, L. Water and Nitrogen Distribution as Affected by Fertigation of Ammonium Nitrate from a Point Source. *Irrig. Sci.* **2003**, *22*, 19–30. [CrossRef]
30. Weslien, P.; Rütting, T.; Kasimir-Klemedtsson, Å.; Klemedtsson, L. Carrot Cropping on Organic Soil Is a Hotspot for Nitrous Oxide Emissions. *Nutr. Cycl. Agroecosystems* **2012**, *94*, 249–253. [CrossRef]
31. de Klein, C.A.M.; van der Weerden, T.J.; Luo, J.; Cameron, K.C.; Di, H.J. A Review of Plant Options for Mitigating Nitrous Oxide Emissions from Pasture-Based Systems. *N. Zeal. J. Agric. Res.* **2020**, *63*, 29–43. [CrossRef]

32. Raposo, E.; Brito, L.F.; Janusckiewicz, E.R.; Oliveira, L.F.; Versuti, J.; Assumpção, F.M.; Cardoso, A.S.; Siniscalchi, D.; Delevatti, L.M.; Malheiros, E.B.; et al. Greenhouse Gases Emissions from Tropical Grasslands Affected by Nitrogen Fertilizer Management. *Agron. J.* **2020**, *112*, 4666–4680. [CrossRef]
33. Sanchez-Martín, L.; Meijide, A.; Garcia-Torres, L.; Vallejo, A. Combination of Drip Irrigation and Organic Fertilizer for Mitigating Emissions of Nitrogen Oxides in Semiarid Climate. *Agric. Ecosyst. Environ.* **2010**, *137*, 99–107. [CrossRef]
34. Ayars, J.E.; Phene, C.J.; Phene, R.C.; Gao, S.; Wang, D.; Day, K.R.; Makus, D.J. Determining Pomegranate Water and Nitrogen Requirements with Drip Irrigation. *Agric. Water Manag.* **2017**, *187*, 11–23. [CrossRef]
35. Hoben, J.P.; Gehl, R.J.; Millar, N.; Grace, P.R.; Robertson, G.P. Nonlinear Nitrous Oxide (N_2O) Response to Nitrogen Fertilizer in on-Farm Corn Crops of the US Midwest. *Glob. Change Biol.* **2011**, *17*, 1140–1152. [CrossRef]
36. Kong, Y.; Watanabe, M.; Nagano, H.; Watanabe, K.; Yashima, M.; Inubushi, K. Effects of Land-Use Type and Nitrogen Addition on Nitrous Oxide and Carbon Dioxide Production Potentials in Japanese Andosols. *Soil Sci. Plant Nutr.* **2013**, *59*, 790–799. [CrossRef]
37. Vadar, H.R.; Pandya, P.A.; Patel, R.J. Effect of Subsurface Drip Irrigation Depth Scheduling in Summer Okra. *Emergent Life Sci. Res.* **2019**, *5*, 52–61. [CrossRef]
38. Singh, D.K.; Rajput, T.B.S. Response of Lateral Placement Depths of Subsurface Drip Irrigation on Okra (*Abelmoschus esculentus*). *Int. J. Plant Prod.* **2012**, *1*, 73–84.